Materials **2014**, *7*, 3867-3880; doi:10.3390/ma7053867

OPEN ACCESS

materials

ISSN 1996-1944

www.mdpi.com/journal/materials

Article

CO_2 Capture and Separation Properties in the Ionic Liquid 1-n-Butyl-3-Methylimidazolium Nonafluorobutylsulfonate

Lingyun Zhou [1,2], Jing Fan [1,*] and Xiaomin Shang [1]

[1] School of Environment, Henan Normal University, Xinxiang 453007, Henan, China; E-Mails: lyzhou1980@163.com (L.Z.); shangxiaomin07@163.com (X.S.)

[2] College of Resource and Environment, Henan Institute of Science and Technology, Xinxiang 453007, Henan, China

* Author to whom correspondence should be addressed; E-Mail: fanjing@henannu.edu.cn; Tel.: +86-373-332-5719; Fax: +86-373-332-9030.

Received: 4 April 2014; in revised form: 4 May 2014 / Accepted: 5 May 2014 / Published: 14 May 2014

Abstract: Recently, the use of ionic liquids (ILs) for carbon capture and separation processes has gained great interest by many researchers due to the high solubility of CO_2 in ILs. In the present work, solubility measurements of CO_2 in the novel IL 1-n-butyl-3-methylimidazolium nonafluorobutylsulfonate $[C_4mim][CF_3CF_2CF_2CF_2SO_3]$ were performed with a high-pressure view-cell technique in the temperature range from 293.15 to 343.15 K and pressures up to about 4.2 MPa. For comparison, solubilities of H_2, N_2, and O_2 in the IL were also measured at 323.15 K via the same procedure. The Krichevsky-Kasarnovsky equation was employed to correlate the measured solubility data. Henry's law constants, enthalpies, and entropies of absorption for CO_2 in the IL were also determined and presented. The CO_2 solubility in this IL was compared with other ILs sharing the same cation. It was shown that the solubility of CO_2 in these ILs follows the sequence: $[C_4mim][CF_3CF_2CF_2CF_2SO_3] \approx [C_4mim][Tf_2N] > [C_4mim][CF_3CF_2CF_2COO] > [C_4mim][BF_4]$, and the solubility selectivity of CO_2 relative to O_2, N_2, and H_2 in $[C_4mim][CF_3CF_2CF_2CF_2SO_3]$ was 8, 16, and 22, respectively. Furthermore, this IL is regenerable and exhibits good stability. Therefore, the IL reported here would be a promising sorbent for CO_2.

Keywords: carbon capture; selectivity; ionic liquid; Krichevsky-Kasarnovsky equation; 1-n-Butyl-3-methylimidazolium nonafluorobutylsulfonate

1. Introduction

The growing CO_2 concentration in the atmosphere compels the scientific community to improve current carbon capture and storage (CCS) technologies, such as membrane-based separation, adsorption, and absorption [1–3]. For this purpose, researchers are extensively involved in the development of novel materials for energy and environmental applications. Among these materials, ionic liquids (ILs) have gained increasing interest because of their outstanding properties over traditional solvents, such as negligible vapor pressures, high thermal and chemical stability, strong solubility capacity, and good recyclability [4]. Among these particular properties, non-volatility potentially makes ILs "green" solvents, because ILs would not contaminate the atmosphere, even in small amounts. Also, tunability of their molecular structures and physicochemical properties are useful characteristics.

Because of these outstanding advantages, ILs have been applied in many research fields, such as analytical chemistry [5], biochemistry [6], electrochemistry [7], catalysis [8], and separation technology [9]. Among these applications, CO_2 separation from post-combustion gas streams attracted significant attention due to CO_2's widely-known contribution to the greenhouse effect. Over the past decades, Blanchard *et al.* [10,11], Anthony *et al.* [12,13], Shariati and Peters [14,15], and Kim *et al.* [16] made extensive contributions to this field. Many ILs, especially the imidazolium ILs, have been successfully synthesized and used for carbon capture [10–20].

In order to improve the solubility of CO_2 in ILs, usually two approaches have been used to optimize the molecular structure of ILs. First, the imidazolium cation was modified by addition of branching chains or some polar groups, such as ether linkages [21] and nitriles [22], to increase the free volume for enhanced CO_2 occupation. Second, a functional CO_2-philic group or anion was introduced by fluorination, carbonylation, or sulfonation to the cation to stabilize the surrounding CO_2 [20,23–25]. Additionally, it was found that the nature of the anions of ILs play a larger role in the solubility of CO_2 than the cations [26–28]. For example, the IL containing highly fluorinated anions, Tris(pentafluoroethyl)trifluorophosphate [FAP^-], was proved to have the highest CO_2 solubility among the ILs with the same cations [29]. Furthermore, C-F bonds were found to have several unique properties, such as increased rigidity and decreased polarity [30]. These properties not only lead to higher gas solubility in highly fluorinated ILs, but also simplify the regeneration of the IL.

The above merits inspired us to combine the two classes of CO_2-philic functional groups, *i.e.*, sulfonation and fluorination phases, together with increasing the C–F bonds to a certain extent to produce the IL 1-n-butyl-3-methylimidazolium nonafluorobutyl sulfonate [C_4mim][$CF_3CF_2CF_2CF_2SO_3$], which was expected to exhibit a higher solubility for CO_2 and an improved energy-saving regeneration. To the best of our knowledge, this is the first time that [C_4mim][$CF_3CF_2CF_2CF_2SO_3$] is used for carbon capture.

In addition to absorption performance and recyclability, the selectivity of ILs is of great importance. Highly efficient separation of CO_2 from other "light" gases (O_2, N_2, H_2, and hydrocarbons) is also a major issue in the CO_2 capture from flue gases. Therefore, the ideal gas solubilities of N_2, O_2, H_2, and CO_2 in the IL were measured in this work. The mole fraction solubility of a single gas in [C_4mim][$CF_3CF_2CF_2CF_2SO_3$] was expressed as Henry's constant, as deduced from the Krichevsky-Kasarnovsky equation. For each gas pair of CO_2 to the three other gases tested, the ideal

solubility selectivity was calculated via Henry's constants to determine if the IL displayed a good ideal gas separation performance. The thermodynamic properties of CO_2 in [C_4mim][$CF_3CF_2CF_2CF_2SO_3$] were also estimated. Additionally, a comparison was made for the solubilities of CO_2 in the studied IL and in the homologues of imidazolium salts to determine the anionic effect.

2. Results and Discussion

2.1. Experimental Solubilities and Anionic Effects of the ILs

In this work, the experimental solubility of CO_2 in [C_4mim][$CF_3CF_2CF_2CF_2SO_3$] was measured in the temperature range from 293.15 to 343.15 K and pressures up to about 4.2 MPa, and the results are shown in Table 1. The same measurements for N_2, O_2, and H_2 were determined at 323.15 K and the results are given in Table 2. Among these experimental data, CO_2 solubilities in [C_4mim][$CF_3CF_2CF_2CF_2SO_3$] are graphically presented in Figure 1 as a function of pressure at different temperatures. The results in Figure 1 show that either a decrease in temperature or an increase in pressure leads to an increase in CO_2 solubility, as typically expected from gas solubility in liquids.

Figure 1. CO_2 solubilities in [C_4mim][$CF_3CF_2CF_2CF_2SO_3$] as a function of pressure at different temperatures: (■, 293.13 K; □, 303.15 K; ▲, 313.15 K;▽, 323.15 K; ●, 313.15 K; ○, 343.15 K). Lines were calculated via the Krichevsky-Kasarnovsky equation.

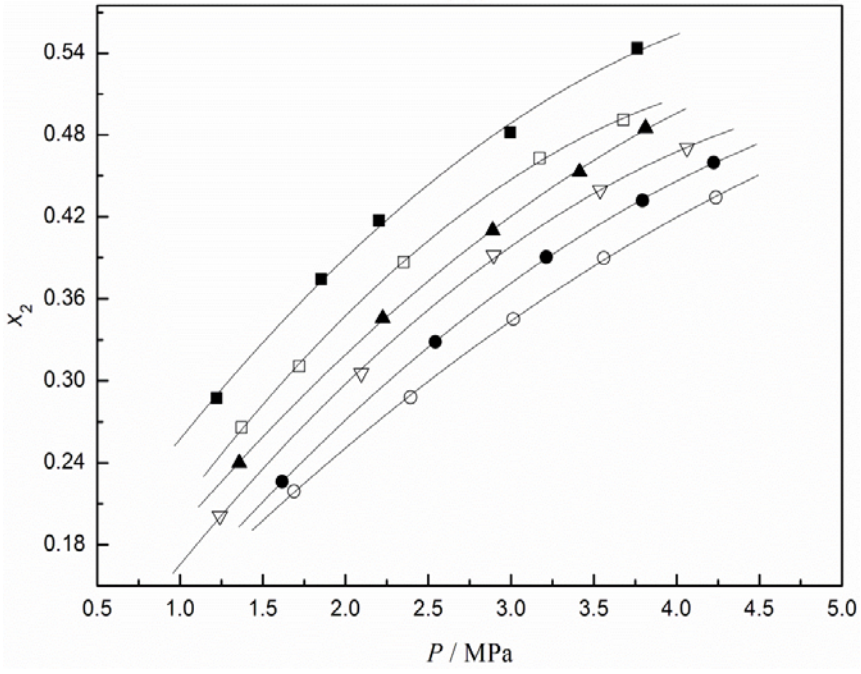

To better understand the absorption performance of CO_2 in [C_4mim][$CF_3CF_2CF_2CF_2SO_3$], we compared CO_2 solubilities in this IL to those in other ILs containing the same cation, as reported in our recent work [31]. These were 1-n-butyl-3-methylimidazolium bis(trifluoromethyl)sulfonylimide ([C_4mim][TF_2N]), 1-n-butyl-3-methylimidazolium heptafluorobutyrate ([C_4mim][$CF_3CF_2CF_2COO$]), and 1-n-butyl-3-methylimidazolium terafluoroborate ([C_4mim][BF_4]). The isotherms of CO_2 in these ILs at 323.15 K are plotted in Figure 2. It can be seen that [C_4mim][$CF_3CF_2CF_2CF_2SO_3$] and [C_4mim][TF_2N] basically exhibited the same solubility values for CO_2, although those in

[C_4mim][$CF_3CF_2CF_2CF_2SO_3$] were slightly greater at higher pressures. The solubility of CO_2 in [C_4mim][$CF_3CF_2CF_2COO$] was somewhat lower than its solubility in [C_4mim][$CF_3CF_2CF_2CF_2SO_3$]. These results suggest that the good capacity of [C_4mim][$CF_3CF_2CF_2CF_2SO_3$] and [C_4mim][TF_2N] for CO_2 adsorption may be attributed to the combination of fluorous alkyl chains and S=O bonds. Also shown in Figure 2 is the solubility of CO_2 in [C_4mim][BF_4], which is generally used as a reference, possessing moderate absorption performance among the imidazolium-based ILs. Clearly, the absorption capacity of CO_2 in the other three ILs is larger than in [C_4mim][BF_4].

Figure 2. Comparison of CO_2 solubility in different ionic liquids at T = 323.15 K: (●, [C_4mim][$CF_3CF_2CF_2CF_2SO_3$]), this work; (□, [C_4mim][TF_2N]), [31]; (△, [C_4mim][$CF_3CF_2CF_2COO$]), [31]; (▼, [C_4mim][BF_4]), [31]. Reproduced with permission from [31]. Copyright 2013 Elsevier.

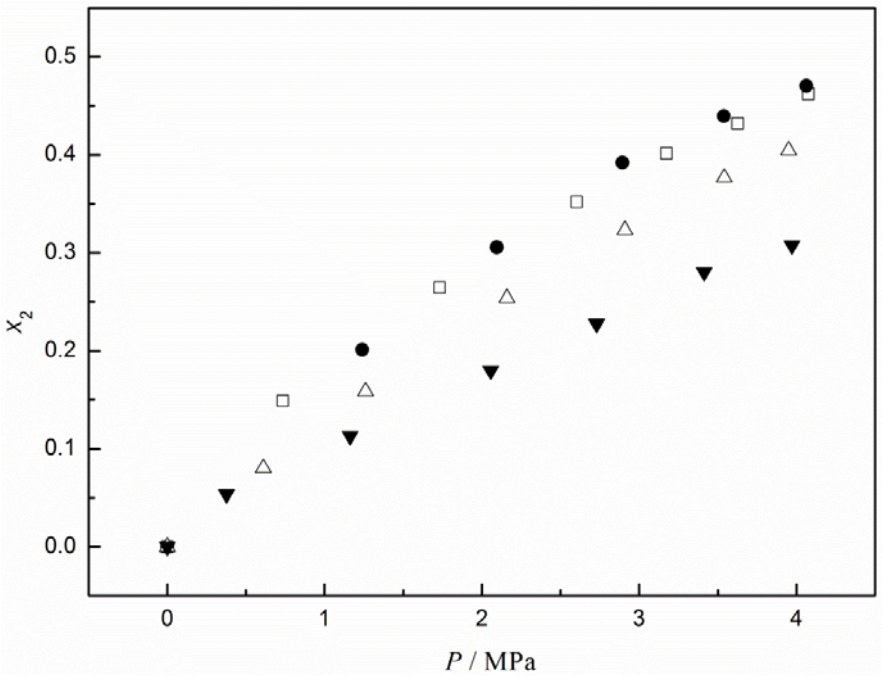

Table 1. Experimental solubility values, expressed as the mole fraction x_2 of CO_2 in [C_4mim][$CF_3CF_2CF_2CF_2SO_3$] at temperature T as a function of pressure P.

P (MPa)	x_2	P (MPa)	x_2	P (MPa)	x_2
T = 293.15 K		**T = 303.15 K**		**T = 313.15 K**	
1.221	0.2831	1.371	0.2659	1.357	0.2399
1.853	0.3837	1.721	0.3128	2.224	0.3458
2.202	0.4261	2.352	0.3867	2.889	0.4101
2.995	0.4989	3.173	0.4631	3.413	0.4529
3.763	0.5436	3.679	0.5022	3.812	0.4851
T = 323.15 K		**T = 333.15 K**		**T = 343.15 K**	
1.240	0.2012	1.617	0.2262	1.689	0.2190
2.095	0.3056	2.543	0.3285	2.393	0.2880
2.894	0.3921	3.213	0.3907	3.014	0.3452
3.538	0.4396	3.795	0.4319	3.560	0.3900
4.063	0.4705	4.224	0.4598	4.238	0.4344

Table 2. Experimental solubility values, expressed as the mole fraction x_2 of N_2, O_2, and H_2 in $[C_4mim][CF_3CF_2CF_2CF_2SO_3]$ at 323.15 K as a function of pressure P.

O_2		N_2		H_2	
***P* (MPa)**	x_2	***P* (MPa)**	x_2	***P* (MPa)**	x_2
2.243	0.0458	2.355	0.0272	2.296	0.0176
4.027	0.0789	4.384	0.0495	4.283	0.02785
5.619	0.1035	5.876	0.0657	5.694	0.0336
6.705	0.1172	6.838	0.0757	6.804	0.03943
8.131	0.1362	8.169	0.0899	7.844	0.04250

2.2. Correlation of the Experimental Data via the Krichevsky-Kasarnovsky Equation

The Krichevsky-Kasarnovsky equation has been widely applied to calculate the solubility of gases in liquid solvents up to high pressures [32–35]. This equation can be described as follows [36]:

$$\ln \frac{f_2(T,P)}{x_2} = \ln H_2^{P_1^S} + \frac{\overline{V}_2^{\infty}\left(P - P_1^S\right)}{RT} \tag{1}$$

where $f_2(T, P)$ is the fugacity of gas solute 2 in the gas phase at pressure P and temperature T; x_2 is the mole fraction of the gas dissolved in the liquid solvents; P_1^S is the saturated vapor pressure of liquid solvents; $\overline{V}_2^{\infty}$ is the partial molar volume of gas at infinite dilution of the liquid solvents; $H_2^{P_1^S}$ is Henry's constant of gas in the liquid solvents at pressure P_1^S , and R is the gas constant. Since the vapor pressure of ILs is negligible, the fugacity of the gas in the gas-IL systems, $f_2(T, P)$, can be substituted for the pure gaseous phase. Thus, the saturated vapor pressure of ionic liquid P_1^S can be considered to be zero. Therefore, Equation (1) can be expressed as:

$$\ln \frac{f_2(T,P)}{x_2} = \ln H_2 + \frac{\overline{V}_2^{\infty}}{RT} P \tag{2}$$

The fugacity of pure gas $f_2(T, P)$ can be obtained according to the following equation:

$$f_2(T,P) = \phi(T,P)P \tag{3}$$

in which ϕ is the fugacity coefficient at pressure P and temperature T, and can be evaluated via the Soave–Redlich–Kwong (SRK) equation of state [37]:

$$P = \frac{RT}{\nu - b} - \frac{a}{\nu(\nu + b)} \tag{4}$$

$$a = 0.42747\left(\frac{R^2T_c^2}{P_c}\right)\alpha(T) \tag{5}$$

$$\alpha(T) = 1 + \beta\left[1 - \left(\frac{T}{T_c}\right)^{0.5}\right] \tag{6}$$

$$\beta = 0.480 + 1.574\omega - 0.176\omega^2 \tag{7}$$

$$b = \frac{0.08664RT}{P_c} \tag{8}$$

$$\ln\phi = Z - 1 - \ln\left[Z\left(1 - \frac{b}{v}\right)\right] - \frac{a\alpha}{bRT}\ln\left(1 + \frac{b}{v}\right) \tag{9}$$

where P is the pressure; T is the temperature; a and b are the constants of the SRK equation of state; v is the molar volume; T_c is the critical temperature and P_c is the critical pressure; $\alpha(T)$ is a temperature-dependent parameter; ω is the acentric factor; and Z is the compressibility factor.

The experimental solubility data in the CO_2/[C_4mim][$CF_3CF_2CF_2CF_2SO_3$] system were correlated with the Krichevsky-Kasarnovsky equation as a function of pressure at different temperatures. For the sake of this, Henry's constants and partial molar volumes of CO_2 at different temperatures should be first obtained. Based on Equation (2), the plot of $\ln(f_2/x_2)$ versus P is given in Figure 3, from which Henry's constant and the partial molar volume of CO_2 at a given temperature were calculated from the intercept and slope of the plot, respectively. At the same time, Henry's constants for O_2, N_2, and H_2 in [C_4mim][$CF_3CF_2CF_2CF_2SO_3$] were also calculated from the experimental solubility data by the same procedure. The obtained values for O_2, N_2, H_2, and CO_2 are listed in Table 3.

From the values of Henry's constants for CO_2 in the IL at different temperatures, the temperature dependence of Henry's constant can be expressed as:

$$\ln\left(H_2/\text{MPa}\right) = 14.7212 - 2709.54/\left(T/K\right) - 0.01434\left(T/K\right) \tag{10}$$

and the plot of lnH_2 *versus* T or $1/T$ is given in Figure 4. The final results for the partial molar volume can be correlated via:

$$V_2^{\infty} / \text{cm}^3 \cdot \text{mol}^{-1} = 453.73 - 0.9678\left(T/K\right) + 0.0014\left(T/K\right)^2 \tag{11}$$

Figure 3. ln(f_{CO2}/x) as a function of pressure at different temperatures: (●, 293.13 K; ○, 303.13 K; ▲, 313.15 K;□, 323.15 K; ■, 333.15 K; ▼, 343.15 K), this work; The lines were calculated via linear regression.

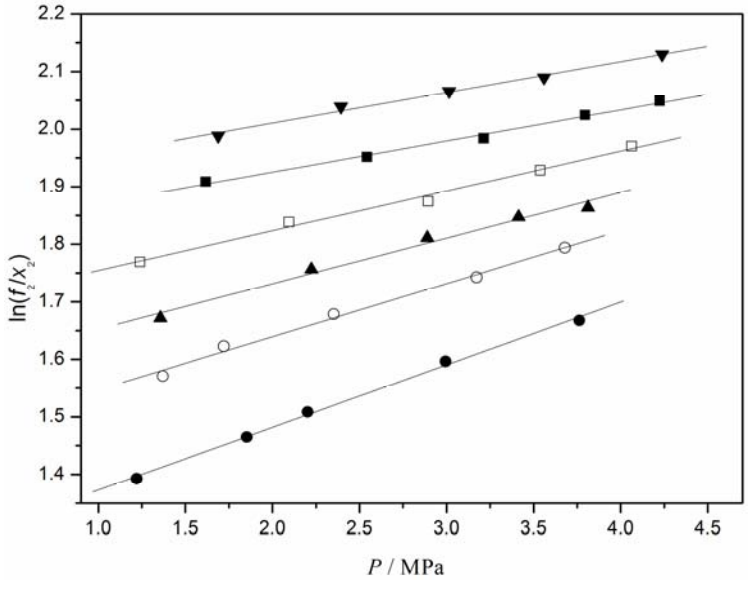

Table 3. Henry's constants H_2 for CO_2, O_2, N_2, and H_2 in $[C_4mim][CF_3CF_2CF_2CF_2SO_3]$ at temperature T and zero pressure [a].

Gas	T (K)	$H_2 \pm \sigma$ (MPa)
CO_2	293.15	3.54 ± 0.03
	303.15	4.39 ± 0.03
	313.15	4.82 ± 0.04
	323.15	5.39 ± 0.03
	333.15	6.16 ± 0.03
	343.15	6.71 ± 0.04
O_2	323.15	44.8 ± 0.8
N_2	323.15	84.8 ± 7
H_2	323.15	116 ± 4

[a] on the mole fraction scale; σ is the standard deviation.

Figure 4. Henry's constants for CO_2 in $[C_4mim][CF_3CF_2CF_2CF_2SO_3]$ at zero pressure and mole fraction scale as a function of the inverse temperature: ■, extrapolated experimental values; –, correlation results.

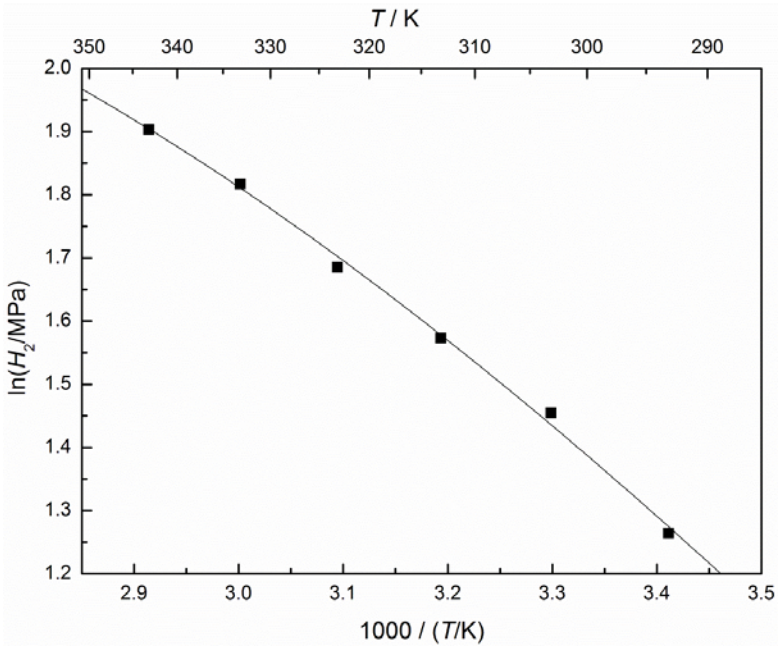

Hence, the experimental solubility values for CO_2 in $[C_4mim][CF_3CF_2CF_2CF_2SO_3]$ at a given temperature and different pressures can be correlated via the Krichevsky-Kasarnovsky equation with Henry's constants given by Equation (10) and the partial molar volume given by Equation (11). The consistency of the obtained correlation values with the experimental solubility data for CO_2 in this IL may be assessed by the average of relative deviation, ARD, defined by:

$$ARD = \frac{1}{n}\sum_{i=1}^{1}\left|\frac{x_{2,i}^{\text{model}} - x_{2,i}}{x_{2,i}}\right| \quad (12)$$

where $x_{2,i}$ is the experimental solubility of CO_2 in [C_4mim][$CF_3CF_2CF_2CF_2SO_3$] in terms of mole fraction and $x_{2,i}^{model}$ is the corresponding value correlated via the Krichevsky-Kasarnovsky equation. The resulting ARD was found to be 0.69%, which is small enough to show that the Krichevsky-Kasarnovsky equation was suitable to describe the solubility behavior of CO_2 with high accuracy in the investigated system.

2.3. Solubility Selectivity and Solution Thermodynamic Properties of CO_2 in the IL

In order to determine the ideal gas separation performance of [C_4mim][$CF_3CF_2CF_2CF_2SO_3$], we compared the values of Henry's law constants for H_2, N_2, O_2, and CO_2 in the IL at 323.15 K (Table 3), and then calculated the ideal solubility selectivity of the gas pairs. As generally known, a low value of Henry's law constant indicates a high gas solubility and vice versa. From Table 3, it can be seen that at the same temperature, the magnitude of Henry's constants for the gases in the IL decreases in the order: $H_2 > O_2 > N_2 > CO_2$, which indicates that the solubility of these gases in the IL follows the sequence: $CO_2 > O_2 > N_2 > H_2$. The solubility selectivity of [C_4mim][$CF_3CF_2CF_2CF_2SO_3$] for CO_2/O_2, CO_2/N_2 and CO_2/H_2 was calculated to be 8, 16, and 22, respectively, which is consistent with the results reported for the other fluorinated ILs in the literature [38].

To examine the reasons why this IL has different absorption performances for these gases, we determined the interactions between the IL and the gas molecules. For comparison, some important structural properties for CO_2, O_2, N_2, and H_2, such as polarizability, dipole moment, and quadrupole moment [39,40], are listed in Table 4. These data clearly indicate that the value of the quadrupole moment of CO_2 is much higher than that of the other three gases. Therefore, we postulated that the higher solubility of CO_2 in the IL was due to the larger quadrupole moment. Additionally, as mentioned earlier, the good solubility of CO_2 in [C_4mim][$CF_3CF_2CF_2SO_3$] could also be ascribed to fluorination and the presence of S=O bonds. On the contrary, the lowest solubility of H_2 in the IL was governed solely by its lowest polarizability. Yet, the fact that O_2 exhibited a higher solubility in the IL than N_2 seems to show that both quadrupole moment and polarizability do not play determinant role in their solubility performances. The behavior of O_2 in the IL might very likely be attributed to the affinity of fluorocarbons for O_2 [41]. Compared to O_2, N_2, and H_2, the significantly higher solubility of CO_2 suggests that it should be possible to capture CO_2 from flue gases.

Table 4. Polarizability (α); dipole moment (μ); and quadrupole moment (*Q*) for CO_2, N_2, O_2, and H_2. Reproduced with permission from [39,40]. Copyright 1999, Prentice Hall PTR and Copyright 1966, Taylor and Francis Group.

Gas	$\alpha \times 10^{24}$ (cm^3)	$\mu \times 10^{18}$ (esu·cm)	$Q \times 10^{26}$ (esu·cm^2)
CO_2	2.64	0	4.3
O_2	1.60	0	0.39
N_2	1.74	0	1.5
H_2	0.81	0	0.662

Additionally, we calculated the thermodynamic properties for the adsorption of CO_2 in [C_4mim][$CF_3CF_2CF_2CF_2SO_3$] using the data of Henry's constants. The partial molar enthalpy and entropy at a specific pressure can be calculated from the following thermodynamic relationships [27]:

$$\Delta H = R\left(\frac{\partial \ln H}{\partial (1/T)}\right)_P \tag{13}$$

$$\Delta S = R\left(\frac{\partial \ln H}{\partial (\ln T)}\right)_P \tag{14}$$

It was found that within the investigated pressure range, the calculated values for ΔH and ΔS were weakly dependent on the pressure and nearly equaled to the values at infinite dilution, as determined via the van 't Hoff equation [27]. From this approximation and aforementioned equations, we obtained values of −11.9 kJ·mol^{-1} for the enthalpy and −40.0 J·mol^{-1}·K^{-1} for the entropy of CO_2 absorption in [C_4mim][$CF_3CF_2CF_2CF_2SO_3$]. These values are very close to those reported for CO_2 in [C_4mim][TF_2N], *i.e.*, −12.5 kJ·mol^{-1} for the enthalpy and −41.3 J·mol^{-1}·K^{-1} for the entropy. This indicates that almost the same strong interactions and structural ordering occurred in these two systems. Considering the fact that these two ILs have the same affinity groups of fluorous alkyl chains and S=O bonds for CO_2, suggested that there would be little difference in the solubilities of CO_2 in these two ILs. This was confirmed by direct comparison of the solubility values of CO_2 in [C_4mim][$CF_3CF_2CF_2CF_2SO_3$] and [C_4mim][Tf_2N], as shown in Figure 2.

In addition, a comparison was made for the heat of absorption of CO_2 in [C_4mim][$CF_3CF_2CF_2CF_2SO_3$] and in non-IL solvents. It was found that the enthalpy value of CO_2 dissolved in the IL is similar to those of CO_2 in conventional organic solvents, such as heptane and ethanol, where physical absorption was observed with absorption enthalpies in the range from −9.7 to −12.8 kJ·mol^{-1} [12]. This suggests that the absorption of CO_2 in [C_4mim][$CF_3CF_2CF_2CF_2SO_3$] is mainly physical absorption in nature, although the ATR-IR study of Kazarian and co-workers [42] indicated possible chemical interactions between the anion and CO_2.

2.4. Recyclability and Reuse of the IL

To evaluate recyclability of the IL, the determination of the absorption capacity of [C_4mim][$CF_3CF_2CF_2CF_2SO_3$] for CO_2 was performed by recycling five times at 323 K. The sample cell containing the IL was pressurized with CO_2 to 1.70 MPa with tiny pressure fluctuations within the five measurements. The pressure fall and corresponding time were monitored and recorded until equilibrium. The amount of dissolved CO_2 in the IL at given time points was calculated on the basis of a pressure-decay observation using the SRK equation of state [25]. In order to explore an energy-efficient method to regenerate the IL, we tried to regenerate the CO_2-saturated IL in two ways. One desorption experiment was performed at 323 K for 1 h by flushing with N_2 at 20 mL·min^{-1}, and, alternatively, by degassing the equilibrium cell at 323 K for 2 h. It was shown that both of the regeneration ways were very efficient. The CO_2 absorption-desorption cycles in [C_4mim][$CF_3CF_2CF_2CF_2SO_3$] by degassing are depicted in Figure 5. It can be seen that the absorption capacities of [C_4mim][$CF_3CF_2CF_2CF_2SO_3$] for CO_2 were quite constant in the five absorption-desorption cycles. Additionally, ^{1}H and ^{13}C NMR studies were conducted for the regenerated IL, and the results showed that no new compounds could be observed during the CO_2 absorption and desorption processes.

Figure 5. CO_2 absorption-desorption cycles in $[C_4mim][CF_3CF_2CF_2CF_2SO_3]$.

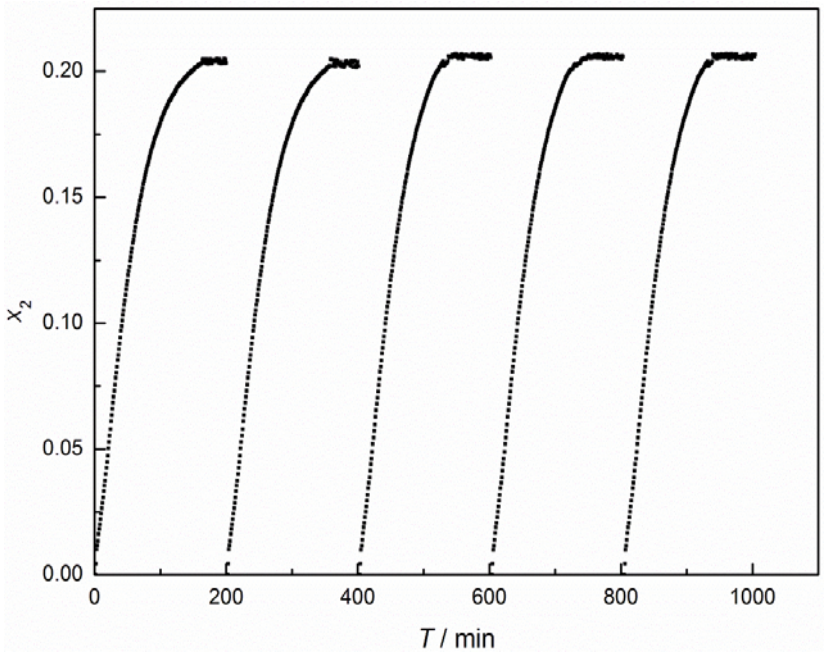

3. Experimental Section

3.1. Materials

The ionic liquid $[C_4mim][CF_3CF_2CF_2CF_2SO_3]$ was obtained from Shanghai Cheng Jie Chem. Co. Ltd (Shanghai, China), with the stated purity no less than 99%. The purchased IL were first dried under vacuum at 323 K for at least 48h and then stored in a vacuum drier before use to prevent it from absorbing water. CO_2, H_2, N_2, and O_2 were purchased from Beijing Paraxair Utility Gas Ltd Co. (Beijing, China) with mass purities of 99.995%, 99.999%, 99.99% and 99.95%, respectively. These gases were used in the experiments without further purification.

3.2. Solubility Experimental Apparatus and Procedure

The detailed experimental apparatus and procedure for the solubility measurements were described previously [31]. The apparatus is schematically depicted in Figure 6. Before the solubility measurements, the volume of the gas tank and total apparatus was determined. In a typical experiment, a known mass of the IL was loaded in the high pressure optical cell, which was placed in a transparent water bath with a magnetic stirrer. The desired temperature was controlled by a temperature controller. Subsequently, the sample cell was evacuated to 10^{-9} bar for 12 h at 323 K to remove dissolved gases and water. After the valve was opened, high pressure gas from the gas storage tank was transferred to the cell for absorption by the IL. Pressure in the system dropped gradually, as observed on the pressure gauge connected to the solubility experimental apparatus. When the pressure remained stable for 1 h, the system was considered to reach a state of equilibrium. The volume of the gas phase at equilibrium could be calculated based on the volume of the IL (volume scale on the optical cell). The gas density of the gas phase in the equilibrated system was determined from the gas mass in the gas tank at

equilibrium divided by the volume of the gas tank. Based on the above parameters, the mass of the gas in the gas phase at equilibrium was determined and consequently the gas mass absorbed by the IL.

Figure 6. Apparatus for the solubility measurements: a, water bath; b, high-pressure cell; c, volume scale; d, magnetic stirring bar; e, magnetic stirrer; f, vacuum pump; g, gas storage tank; h, needle valve; P, pressure gauge.

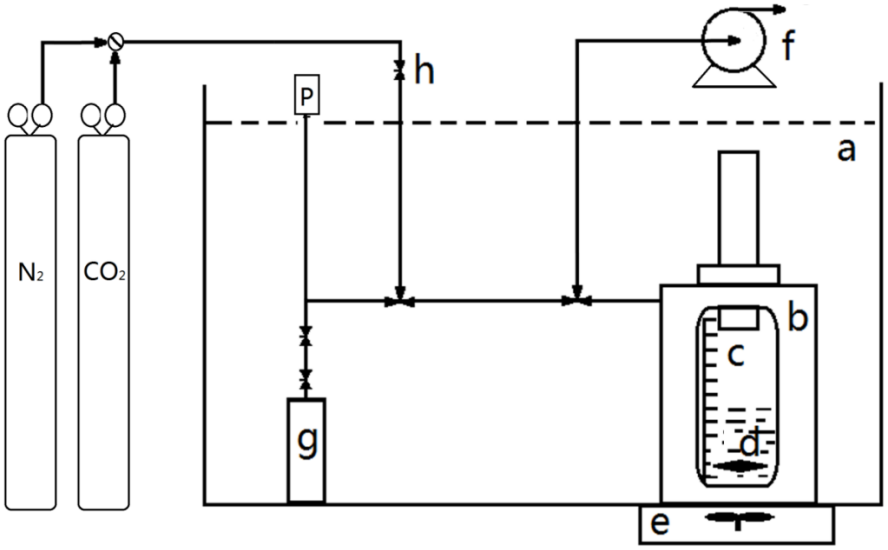

The mass of gas and IL was determined with an electronic balance with a precision of ±0.0001 g. The temperature of the solubility experiments controlled by a temperature controller was within an uncertainty of ±0.1 K. Gas pressures with a precision of ±0.001 MPa were measured with a pressure gauge in the range from 0 to 10 MPa. The IL volume read from the volume scale on the optical cell was within the precision of ±0.02 mL. All data shown in the tables and figures were the average of at least three trials. From the error analysis, the estimated uncertainty in the solubility is ±0.8%.

4. Conclusions

In this work, we reported the solubilities of CO_2, O_2, N_2, and H_2 in $[C_4mim][CF_3CF_2CF_2CF_2SO_3]$ and compared the CO_2 solubility in this IL to other 1-butyl-3-methylimidazolium-based ILs. It was found that $[C_4mim][CF_3CF_2CF_2CF_2SO_3]$ has a comparable ability for CO_2 capture to $[C_4mim][TF_2N]$ due to a combination of fluorination and the presence of S=O bonds. By using the Krichevsky-Kasarnovsky equation, Henry's constants of CO_2, O_2, N_2, and H_2 in the IL were determined and solution thermodynamic properties for IL/CO_2 system were derived. The solubility selectivity of $[C_4mim][CF_3CF_2CF_2CF_2SO_3]$ for each gas pair tested was calculated from their corresponding Henry's constants. It was shown that the values for CO_2/O_2, CO_2/N_2, and CO_2/H_2 were 8, 16, and 22, respectively. Also, the large affinity of the IL for CO_2 was explained by more favorable interactions between the gas and the IL molecules. In addition, the gas solubility expressed as mole fraction at given temperature and pressure was correlated via the Krichevsky-Kasarnovsky equation with an average relative deviation of about 0.69% for the system of $CO_2/[C_4mim][CF_3CF_2CF_2CF_2SO_3]$. We estimate that the present study will aid in the design of promising absorbents for CO_2 by estimating both the absorption capacity and the selectivity.

Acknowledgments

We gratefully acknowledge the support from the National Natural Science Foundation of China (Grant No. 21377036).

Author Contributions

The research work outlined in this publication was performed by Lingyun Zhou, Jing Fan and Xiaomin Shang. The study was designed by Jing Fan and Lingyun Zhou, the experiments were carried out by Lingyun Zhou and Xiaomin Shang, and the initial manuscript was prepared by Lingyun Zhou. Analysis of experimental results was performed by Jing Fan and Lingyun Zhou, and revision of the manuscript was performed by Jing Fan.

Conflicts of Interest

The authors declare no conflict of interest.

References

1. Henni, A.; Li, J.; Tontiwachwuthikul, P. Reaction kinetics of CO_2 in aqueous 1-amino-2-propanol, 3-amino-1-propanol, and dimethylmonoethanolamine solutions in the temperature range of 298–313 K using the stopped-flow technique. *Ind. Eng. Chem. Res.* **2008**, *47*, 2213–2220.
2. Li, Y.; Sun, N.; Li, L.; Zhao, N.; Xiao, F.; Wei, W.; Sun, Y.; Huang, W. Grafting of amines on ethanol-extracted SBA-15 for CO_2 adsorption. *Materials* **2013**, *6*, 981–999.
3. Bermúdez, J.; Dominguez, P.; Arenillas, A.; Cot, J.; Weber, J.; Luque, R. CO_2 separation and capture properties of porous carbonaceous materials from leather residues. *Materials* **2013**, *6*, 4641–4653.
4. Brennecke, J.F.; Gurkan, B.E. Ionic liquids for CO_2 capture and emission reduction. *J. Phys. Chem. Lett.* **2010**, *1*, 3459–3464.
5. Berthod, A.; Ruiz-Angel, M.; Carda-Broch, S. Ionic liquids in separation techniques. *J. Chromatogr. A* **2008**, *1184*, 6–18.
6. Freemantle, M. *An Introduction to Ionic Liquids*; Royal Society of Chemistry: London, UK, 2010; pp 214-229.
7. Buzzeo, M.C.; Evans, R.G.; Compton, R.G. Non-haloaluminate room-temperature ionic liquids in electrochemistry—A review. *ChemPhysChem* **2004**, *5*, 1106–1120.
8. Pârvulescu, V.I.; Hardacre, C. Catalysis in ionic liquids. *Chem. Rev.* **2007**, *107*, 2615–2665.
9. Blanchard, L.A.; Brennecke, J.F. Recovery of organic products from ionic liquids using supercritical carbon dioxide. *Ind. Eng. Chem. Res.* **2001**, *40*, 287–292.
10. Blanchard, L.A.; Hancu, D.; Beckman, E.J.; Brennecke, J.F. Green processing using ionic liquids and CO_2. *Nature* **1999**, *399*, 28–29.
11. Blanchard, L.A.; Gu, Z.; Brennecke, J.F. High-pressure phase behavior of ionic liquid/CO_2 systems. *J. Phys. Chem. B* **2001**, *105*, 2437–2444.

12. Anthony, J.L.; Maginn, E.J.; Brennecke, J.F. Solubilities and thermodynamic properties of gases in the ionic liquid 1-n-butyl-3-methylimidazolium hexafluorophosphate. *J. Phys. Chem. B* **2002**, *106*, 7315–7320.
13. Anthony, J.L.; Crosthwaite, J.M.; Hert, D.G.; Aki, S.N.; Maginn, E.J.; Brennecke, J.F. Phase equilibria of gases and liquids with 1-n-butyl-3-methylimidazolium tetrafluoroborate. *ACS Symp. Ser.* **2003**, *856*, 110–120.
14. Shariati, A.; Peters, C.J. High-pressure phase behavior of systems with ionic liquids: II. The binary system carbon dioxide+1-ethyl-3-methylimidazolium hexafluorophosphate. *J. Supercrit. Fluids* **2004**, *29*, 43–48.
15. Shariati, A.; Peters, C.J. High-pressure phase equilibria of systems with ionic liquids. *J. Supercrit. Fluids* **2005**, *34*, 171–176.
16. Kim, Y.S.; Choi, W.Y.; Jang, J.H.; Yoo, K.P.; Lee, C.S. Solubility measurement and prediction of carbon dioxide in ionic liquids. *Fluid Phase Equilibria* **2005**, *228–229*, 439–445.
17. Yokozeki, A.; Shiflett, M.B.; Junk, C.P.; Grieco, L.M.; Foo, T. Physical and chemical absorptions of carbon dioxide in room-temperature ionic liquids. *J. Phys. Chem. B* **2008**, *112*, 16654–16663.
18. Shiflett, M.B.; Yokozeki, A. Phase Behavior of Carbon Dioxide in Ionic Liquids: [emim][Acetate], [emim][Trifluoroacetate], and [emim][Acetate] + [emim][Trifluoroacetate] Mixtures. *J. Chem. Eng. Data* **2008**, *54*, 108–114.
19. Taib, M.M.; Murugesan, T. Solubilities of CO_2 in aqueous solutions of ionic liquids (ILs) and monoethanolamine (MEA) at pressures from 100 to 1600 kPa. *Chem. Eng. J.* **2012**, *181–182*, 56–62.
20. Almantariotis, D.; Gefflaut, T.; Pádua, A.A.H.; Coxam, J.Y.; Costa Gomes, M.F. Effect of fluorination and size of the alkyl side-chain on the solubility of carbon dioxide in 1-Alkyl-3-methylimidazolium bis(trifluoromethylsulfonyl)amide ionic liquids. *J. Phys. Chem. B* **2010**, *114*, 3608–3617.
21. Bara, J.E.; Gabriel, C.J.; Lessmann, S.; Carlisle, T.K.; Finotello, A.; Gin, D.L.; Noble, R.D. Enhanced CO_2 separation selectivity in oligo(ethylene glycol) functionalized room-temperature ionic liquids. *Ind. Eng. Chem. Res.* **2007**, *46*, 5380–5386.
22. Mota-Martinez, M.T.; Althuluth, M.; Kroon, M.C.; Peters, C.J. Solubility of carbon dioxide in the low-viscosity ionic liquid 1-hexyl-3-methylimidazolium tetracyanoborate. *Fluid Phase Equilibria* **2012**, *332*, 35–39.
23. Baltus, R.E.; Culbertson, B.H.; Dai, S.; Luo, H.; DePaoli, D.W. Low-pressure solubility of carbon dioxide in room-temperature ionic liquids measured with a quartz crystal microbalance. *J. Phys. Chem. B* **2003**, *108*, 721–727.
24. Muldoon, M.J.; Aki, S.N.V.K.; Anderson, J.L.; Dixon, J.K.; Brennecke, J.F. Improving carbon dioxide solubility in ionic liquids. *J. Phys. Chem. B* **2007**, *111*, 9001–9009.
25. Lee, H.; Cho, M.H.; Lee, B.S.; Palgunadi, J.; Kim, H.; Kim, H.S. Alkyl-fluoroalkylimidazolium-based ionic liquids as efficient CO_2 absorbents. *Energy Fuels* **2010**, *24*, 6689–6692.
26. Aki, S.N.V.K.; Mellein, B.R.; Saurer, E.M.; Brennecke, J.F. High-pressure phase behavior of carbon dioxide with imidazolium-based ionic liquids. *J. Phys. Chem. B* **2004**, *108*, 20355–20365.
27. Anthony, J.L.; Anderson, J.L.; Maginn, E.J.; Brennecke, J.F. Anion effects on gas solubility in ionic liquids. *J. Phys. Chem. B* **2005**, *109*, 6366–6374.

28. Bara, J.E.; Carlisle, T.K.; Gabriel, C.J.; Camper, D.; Finotello, A.; Gin, D.L.; Noble, R.D. Guide to CO_2 separations in imidazolium-based room-temperature ionic liquids. *Ind. Eng. Chem. Res.* **2009**, *48*, 2739–2751.
29. Almantariotis, D.; Stevanovic, S.; Fandiño, O.; Pensado, A.S.; Padua, A.A.H.; Coxam, J.Y.; Costa Gomes, M.F. Absorption of carbon dioxide, nitrous oxide, ethane and nitrogen by 1-Alkyl-3-methylimidazolium (Cnmim, n = 2,4,6) Tris(pentafluoroethyl)trifluorophosphate Ionic liquids (eFAP). *J. Phys. Chem. B* **2012**, *116*, 7728–7738.
30. Costa Gomes, M.F.; Pádua, A.A.H. Interactions of carbon dioxide with liquid fluorocarbons. *J. Phys. Chem. B* **2003**, *107*, 14020–14024.
31. Zhou, L.; Fan, J.; Shang, X.; Wang, J. Solubilities of CO_2, H_2, N_2 and O_2 in ionic liquid 1-n-butyl-3-methylimidazolium heptafluorobutyrate. *J. Chem. Thermodyn.* **2013**, *59*, 28–34.
32. Yuan, X.; Zhang, S.; Liu, J.; Lu, X. Solubilities of CO_2 in hydroxyl ammonium ionic liquids at elevated pressures. *Fluid Phase Equilibria* **2007**, *257*, 195–200.
33. Zhao, Y.; Zhang, X.; Dong, H.; Zhen, Y.; Li, G.; Zeng, S.; Zhang, S. Solubilities of gases in novel alcamines ionic liquid 2-[2-hydroxyethyl (methyl) amino] ethanol chloride. *Fluid Phase Equilibria* **2011**, *302*, 60–64.
34. Althuluth, M.; Mota-Martinez, M.T.; Kroon, M.C.; Peters, C.J. Solubility of carbon dioxide in the ionic liquid 1-Ethyl-3-methylimidazolium Tris(pentafluoroethyl)trifluorophosphate. *J. Chem. Eng. Data* **2012**, *57*, 3422–3425.
35. Sakhaeinia, H.; Jalili, A.H.; Taghikhani, V.; Safekordi, A.A. Solubility of H_2S in ionic liquids 1-Ethyl-3-methylimidazolium Hexafluorophosphate ([emim][PF_6]) and 1-Ethyl-3-methylimidazolium Bis (trifluoromethyl) sulfonylimide ([emim][Tf_2N]). *J. Chem. Eng. Data* **2010**, *55*, 5839–5845.
36. Krichevsky, I.R.; Kasarnovsky, J.S. Thermodynamical calculations of solubilities of nitrogen and hydrogen in water at high pressures. *J. Am. Chem. Soc.* **1935**, *57*, 2168–2171.
37. Cheng, K.-W.; Tang, M.; Chen, Y.-P. Vapor–Liquid equilibria of carbon dioxide with diethyl oxalate, ethyl laurate, and dibutyl phthalate binary mixtures at elevated pressures. *Fluid Phase Equilibria* **2001**, *181*, 1–16.
38. Camper, D.; Bara, J.; Koval, C.; Noble, R. Bulk-fluid solubility and membrane feasibility of rmim-based room-temperature ionic liquids. *Ind. Eng. Chem. Res.* **2006**, *45*, 6279–6283.
39. Prausnitz, J.M.; Lichtenthaler, R.N.; de Azevedo, E.G. *Molecular Thermodynamics of Fluid Phase Equilibria*, 3rd ed.; Prentice-Hall: Upper Saddle River, NJ, USA, 1999.
40. Stogryn, D.E.; Stogryn, A.P. Molecular multipole moments. *Mol. Phys.* **1966**, *11*, 371–393.
41. Wesseler, E.P.; Iltis, R.; Clark, L.C., Jr. The solubility of oxygen in highly fluorinated liquids. *J. Fluor. Chem.* **1977**, *9*, 137–146.
42. Kazarian, S.G.; Briscoe, B.J.; Welton, T. Combining ionic liquids and supercritical fluids: ATR-IR study of CO_2 dissolved in two ionic liquids at high pressures. *Chem. Commun.* **2000**, *2000*, 2047–2048.